Nanoscale Advances

ROYAL SOCIETY OF CHEMISTRY

PAPER

View Article Online
View Journal | View Issue

Cite this: *Nanoscale Adv.*, 2022, **4**, 2823

Architectural design of core–shell nanotube systems based on aluminosilicate clay

Anna Stavitskaya, *[a] Maria Rubtsova, [a] Aleksandr Glotov, [a] Vladimir Vinokurov,[a] Anna Vutolkina,[b] Rawil Fakhrullin [c] and Yuri Lvov *[d]

A nanoarchitectural approach to the design of functional nanomaterials based on natural aluminosilicate nanotubes and their catalysis, and practical applications are described in this paper. We focused on the buildup of hybrid core–shell systems with metallic or organic molecules encased in aluminosilicate walls, and nanotube templates for structured silica and zeolite preparation. The basis for such an architectural design is a unique Al_2O_3/SiO_2 dual chemistry of 50 nm diameter halloysite tubes. Their structure and site dependent properties are well combined with biocompatibility, environmental safety, and abundant availability, which makes the described functional systems scalable for industrial applications. In these organic/ceramic hetero systems, we outline drug, dye and chemical inhibitor loading inside the clay nanotubes, accomplished with their silane or amphiphile molecule surface modifications. For metal–ceramic tubule composites, we detailed the encapsulation of 2–5 nm Au, Ru, Pt, and Ag particles, Ni and Co oxides, NiMo, and quantum dots of CdZn sulfides into the lumens or their attachment at the outside surface. These metal–clay core–shell nanosystems show high catalytic efficiency with increased mechanical and temperature stabilities. The combination of halloysite nanotubes with mesoporous MCM-41 silica allowed for a synergetic enhancement of catalysis properties. Finally, we outlined the clay nanotubes' self-assembly into organized arrays with orientation and ordering similar to nematic liquid crystals, and these systems are applicable for life-related applications, such as petroleum spill bioremediation, antimicrobial protection, wound healing, and human hair coloring.

Received 15th March 2022
Accepted 17th April 2022

DOI: 10.1039/d2na00163b

rsc.li/nanoscale-advances

1. Introduction

The nanoarchitectonics concept is prominent in the design of composite materials using nanoscale units (macromolecules or atom clusters). The production of such functional nanomaterials *via* architectural approaches uses a combination of methods including synthesis, atom/molecular manipulation, self-organization accomplished with an externally controlled assembly, micro-fabrication, and biomimetic processes.[1] Nanoarchitectonics opens new perspectives in constructing materials with tunable properties for medicine, microbiology, photonics, electronics, catalysis, and smart chemical composites. Examples of such methods may be found in Langmuir–Blodgett and layer-by-layer assembly, producing multicomponent chemical "sandwich-like" films and coatings[2] in complex organic micro-capsules allowing for targeted and controlled drug delivery,[3] and in other core–shell systems, often containing gold coated with thiol based organic shells or bimetallic nanoparticles.[4] Here, we describe the design of tubule core–shell halloysite clay structures.[5–9]

Halloysite tubule clay is an environmentally safe, biocompatible nanomaterial, and it is abundantly available from natural deposits. It has a diameter from 50 to 90 nm, depending on the source, with an internal lumen diameter from 10 to 25 nm and a length of *ca.* 1 μm, Fig. 1. Halloysite nanotubes with the chemical formula $Al_2Si_2O_5(OH)_4 \cdot nH_2O$ are formed by the rolling of aluminosilicate sheets, giving the tubes a wall of 15–20 layers with 0.72 nm periodicity in their dry state. Such tubes have an external surface composed of tetrahedral siloxane (Si–O–Si) groups, and an inner lumen surface consisting of octahedral aluminol (Al–OH) groups. This clay with SiO_2 on the external surface and Al_2O_3 inside is a unique example of nanotubes having different external and internal surfaces, which allows for selective chemical modification of their interior and exterior.[6,7] The simplest of which is an electrostatic approach using a surface charge (zeta-potential) of *ca.* +20 mV on the inner surface in a pH range of 4–8 (efficient for loading of negative chemicals), and an external −30 mV silica surface for adsorption of positively charged components.

The dual tubes' charging allows for spontaneous loading of negatively charged components inside the halloysite tubes. This

[a]*Department of Physical and Colloid Chemistry, Gubkin Russian State University of Oil and Gas, Moscow, 119991, Russian Federation. E-mail: stavitsko@mail.ru*

[b]*Chemistry Department, M. Lomonosov Moscow State University, Moscow, 119991, Russian Federation*

[c]*Bionanotechnology Lab, Institute of Fundamental Medicine and Biology, Kazan Federal University, Kazan, Republic of Tatarstan, 420008, Russian Federation*

[d]*Institute for Micromanufacturing, Louisiana Tech University, Ruston, LA 71272, USA. E-mail: ylvov@latech.edu*

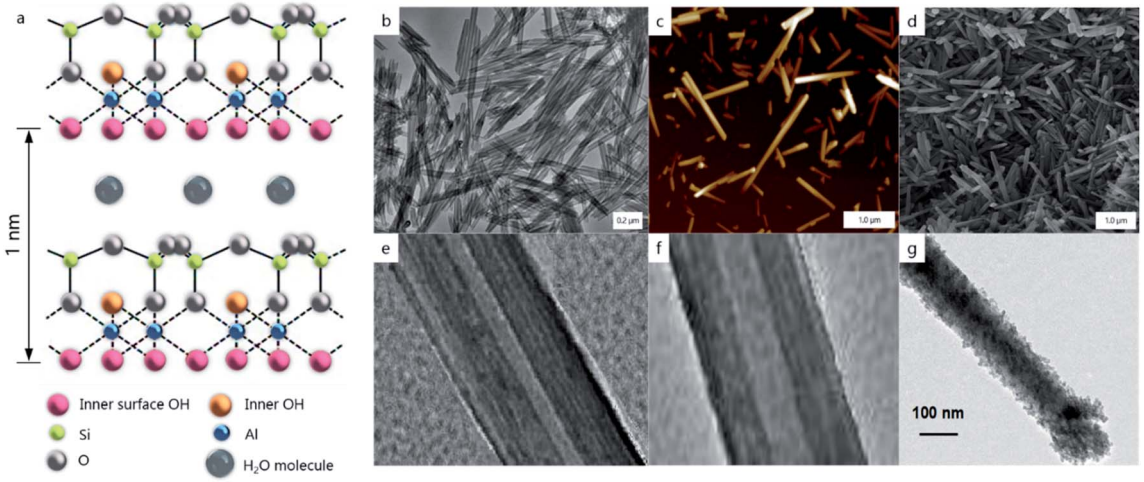

Fig. 1 Schematics of the tube wall composition (a), and TEM, AFM and SEM images of pristine halloysite nanotubes, the samples provided by Applied Minerals Inc, USA, (b–d) and TEM images of increasing halloysite lumen diameter from 12 to 25 nm with sulphuric acid etching (e and f); the nanotube LbL-coated with (polyethyleneimine/7 nm silica)$_2$ shell (g), adapted from ref. 7 with permission from Wiley, copyright 2016.

approach is convenient for the encapsulation of drugs, proteins, and DNA, which are mostly negatively charged. The loading of bioactive compounds inside the halloysite nanotubes was the first example of core–shell organic/inorganic tubule clay architecture.[7] Pristine halloysite allows for up to 11 wt% drug loading inside the tube; however, acid etching increases the lumen diameter to 25 nm and thus quadruples the loading efficiency to 40 wt%, which is close to that of polymeric microcapsules.[7] Typically, after drug loading and drying, halloysite may remain intact for years and then be used in medical formulations like creams, implants or tablets. The release time of water-soluble drugs from such a formulation is 10–20 hours; however, it may be extended to weeks and months by the encapsulation of loaded tubes *via* a layer-by-layer method, and with dextran or fatty acid capping. Incorporating antibiotic loaded nanotubes in electrospun microfibers or bone implants increased drug release time to 2–3 weeks.[10,11]

Halloysite is safe for cell cultures at less than 0.2 mg mL^{-1}, and is capable of being absorbed by biological cells and macrophages. Mice orally treated for three months with daily concentrations of 0.1 g kg^{-1} of body mass displayed minor liver toxicity, but smaller halloysite concentrations were safe. This safe dose corresponds to a possibility for a human to consume 2–3 grams of halloysite daily in tablet formulations for months without harmful consequences, though inhalation may be dangerous at lower concentrations.[12–14] In our opinion, drug loaded halloysite may be used mostly in oral or topical applications or in muscle injections, but its use in blood vein administration is hardly possible because these nanotubes are not biodegradable.

An interesting case of a bioactive core–shell system is the clay nanotubes loaded with enzymes. Biocatalytic activity of encased proteins was stabilized against high pH and temperature, and such aqueous encapsulation is promising for enzymatic catalysis in non-water surroundings.[15,16]

Methods of halloysite nanotube external coating are based on silane binding to its silica surface. This allows us to use the power of well elaborated silane chemistry in halloysite outer modification, allowing the use of different endings of silane compounds and making the nanotube surface partially and fully hydrophobic, or providing amines for further surface reactivity.[7,17,18] Quite efficient was also the nanotube coating with polydopamine possessing photothermic properties. The nanotubes' lumens were loaded with natural antibacterial carvacrol and lauric acid ($C_{12}H_{24}O_2$) having a melting temperature of 43 °C. Therefore, this loaded photo-sensitive core system had the stoppers which were trigger-opened under laser irradiation, due to elevated temperatures releasing the encapsulated carvacrol.[19] The idea of the tubes' inner clogging or end stoppers is attractive for switchable release; this was also used for halloysite anticorrosion loading and for biodegradable stoppers in intracellular drug delivery.[7,9,10]

A difficult, but very promising concept, is the formation of metal (catalytic) particles inside the clay nanotubes. In some cases, one can successfully load metal salts such as silver acetate or molybdate tetrahydrate ($(NH_4)_6Mo_7O_{24}$) for metal core production. However, we generally must load into the positively charged tube's lumen cationic metal ions at pH 4–9 to overcome electrostatic repulsion. In this case, the lumen surface pretreatment is needed to neutralize the internal charge, involving additional stronger chemical bonding.[20–22] Adsorption of cations on a negatively charged nanotube surface for external shell formation is a way to obtain halloysite metal shells.[7] Finally, more sophisticated architectural designs are involved in the formation of different types of particles inside and outside the nanotubes for synergistically enhanced bimetallic catalysis.[8] In Section 2, we will discuss these multicomponent hierarchical core–shell nanosystems.

Scheme 1 presents our vision of architectures based on these aluminosilicate nanotubes. In the first step, one can selectively modify halloysite tubes outside or inside. Then, using space-confined activation, one can grow porous mesosilica or bind preformed metal nanoparticles (*e.g.* gold by the thiol ending reaction) to a silane pretreated surface.[8,23] We can load metal

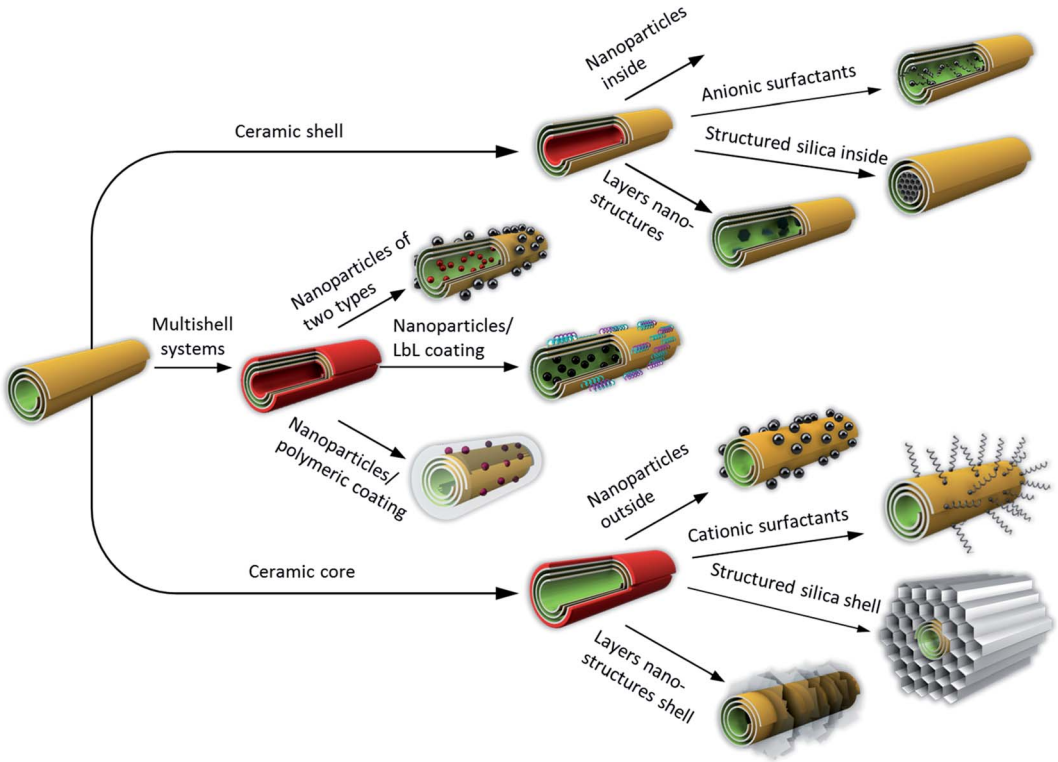

Scheme 1 Architectural approach in core–shell systems based on clay nanotubes' inside/outside modification with metal particles (round and platelets), outermost hydrophobization and mesosilica formation.

ions onto or into the tubes with further reduction to get 2–5 nm metal particles seeded outside or inside the clay. It is easier to accumulate cationic metal ions onto the negative outer tubes' surface, so that in many cases one can perform a nanoparticle formation reaction in the presence of halloysite to get well-seeded ceramic core–metal shell systems.[8,20] It is a simple and efficient reaction; the only problem is ensuring the stability of particle attachment to the tube surface, for example, for multiple catalysis applications. Metal core systems may be transposed to practical catalytic systems by hydrophobic finishing with alkyltriethoxysilanes of 8–18 carbon atoms on the outer halloysite surface.[8] This hydrophobized metal–ceramic material is a promising template for the placement of ruthenium into the lumens, resulting in efficient catalysts for water–petroleum mixtures. A water contact angle of 122° was reached for these hybrid systems, which resulted in the shielding of embedded metals from leaching and water deactivation.

One of the trends in new functional materials based on halloysite nanotubes is the formation of structured silica on their outer or inner surfaces. Pristine halloysite has a specific surface area of 60–70 $m^2\ g^{-1}$, and pores in the range of 10–15 nm with low acidity that impede its usage in organic catalysis. The surface area could be moderately increased by alumina acid etching or drastically enhanced by selective adherence of smaller-pore silica, such as MCM-41 (Mobil Composite Material-41) or nanocarbon (Scheme 1, bottom right).[8,23–26] Negatively charged nanotube outer surfaces were modified with cationic surfactants, *e.g.* quaternary ammonium salts such as cetyltrimethyl ammonium bromide.[26] Following the first attached amphiphile layer, bulk surfactant multilayers were formed, and after silica hydrolysis it led to the formation of an inorganic composite with a silica shell and hollow halloysite in the middle (the surfactant was removed by etching or calcination at 550 °C). This hierarchical material is characterized by a high specific surface area of 700 $m^2\ g^{-1}$, bimodal pore size distribution (2–3 nm for silica and 10–15 nm for halloysite), enhanced acidity, and mechanical and thermal stabilities.[8,26] A reversed strategy is used by placing mesoporous silica inside the nanoclay lumen, starting with the pore de-alumination by acid treatment, selective inner adsorption of anionic surfactants, and formation of mesoporous silica inside the tubes with the same procedure as described above. In Section 3, we give detailed results on the two-compound nanosystem construction, including their scaled-up modification based on the spray-based architecture of halloysite-mesosilica microbeads.

In Section 4, we will discuss the formation of oriented arrays of the clay nanotubes. The mechanism of ordering is based on the electrostatic repulsion of the charged nanorods inducing their orientation, which is fixed by the tubes' condensation and drying. There is some similarity in the nanotube array formation with ordering in nematic liquid crystals, proved by similar optical phenomena by polarized microscopy. Such a nanotube orientation may be achieved at the edge of dried nanoclay droplets as the "coffee-ring" phenomenon, in capillary, microchannels, and even with simple halloysite brash coatings. Halloysite nanotubes were also assembled at the oil–water interface

based on the mechanisms of Pickering emulsification.[7,9] With a unique halloysite tubular structure, its different inside/outside chemistry, abundant natural deposits and ecological safety, this clay aluminosilicate is a prospective platform for nanoarchitectonic design of new functional materials with a wide range of applications, from pharmacological and biomedical to large scale petrochemical catalysis and spill oil remediation.

2. Selective metal modification inside and outside the tubes

Halloysite architecture is a promising approach to the formation of selective, efficient and stable (under harsh conditions) catalysts. For this, we utilized the following strategies: (1) the clay tube's outer surface is coated with metals or their composites; (2) formation of a metal core in the tube's lumen; and (3) multi-shell system design, as shown in Scheme 2.[8,20] In most cases, the metal inside the nanotubes is presented as 2–4 nm diameter particles, but it was also possible to synthesize inner nanorods, like for silver or cobalt oxide fillings, Fig. 2.[7,20] Selective inner loading was demonstrated for Ru-particles formed within azine-modified halloysite cavities, including lumens and slit defects in the tube walls. Gold nanoparticle peapods were synthesized inside halloysite lumens in a nonpolar solvent using surfactant pre-treatment.[21]

Self-assembly provides a pathway to the design of integrated scale (nano/micro/macro) organic–ceramic–metal systems.[27] Nanoflake or nanosheet tube shells could be obtained under favorable conditions when layer structures, like metal sulfides, are synthesized. Ultrathin NiO nanosheets assembled onto pristine clay tubes through a simple precipitation reaction were also reported.[28,29] In_2S_3 plates were stabilized on the surface of azine-modified clay using microwave irradiation and polyethylene oxide as a solvent.[9] We demonstrated MoS_2 multilayer organization in lumens of halloysite *via* hydrothermal synthesis.

Quantum dots of various compositions with tunable spectral characteristics were produced. On halloysite, 3–5 nm diameter ZnS, CdS and $Cd_{x-1}Zn_xS$ particles were synthesized selectively inside and outside the clay nanotubes by ligand assisted binding, Fig. 2. Grafting agents (with a silane or azine ligand) play a significant role in the stabilization of photo systems prepared with halloysite as a quantum dot carrier. For example, the nanotube silane grafting enhances the fluorescence of inner-located CdS nanoparticles, while decreasing their photocatalytic hydrogen production.[30] Stabilization of CdS quantum dots synthesized on the surface of the clay nanotubes *via* azine-assisted grafting showed an enhanced photocatalytic reaction in hydrogen production.[31]

By variation of synthesis parameters, one can produce bright colored and biosafe nanoclay markers for cell labeling.[31,32] Such nanotubes with incased quantum dots showed low toxicity to eukaryotic cells and to model nematodes such as *C. elegans*. CdSe quantum dots were selectively loaded inside the nanoclay lumens driven by the electrostatic interaction of negatively charged CdSe particles and positively charged lumens (Fig. 2).[33]

To achieve selective loading of metal containing compounds, an interesting approach was reported by modifying the tube lumen with sodium alkylsulphates to create tubular inorganic micelles for efficient catalysts.[34] A similar strategy was employed to synthesize CoMoS nanoparticles embedded into halloysite. It resulted in the formation of dispersible clay nanoreactors for hydrotreating of straight run diesel. This strategy is based on electrostatic interaction between anionic $PMo_{12}O_{40}^{3-}$ species and the positively charged halloysite inner cavity, which drives Co and Mo ions to the lumen followed by high-temperature

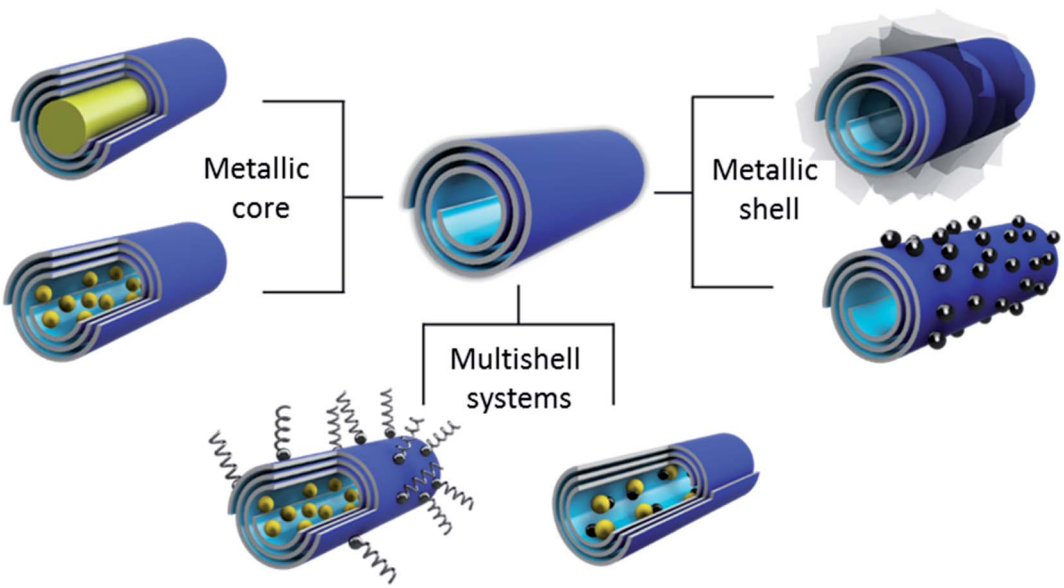

Scheme 2 Metal–ceramic core–shell tubule system synthesis strategies: metal cores of nanorods and balls, metal shells of plates and balls, and metal load within a hydrophobized clay shell.

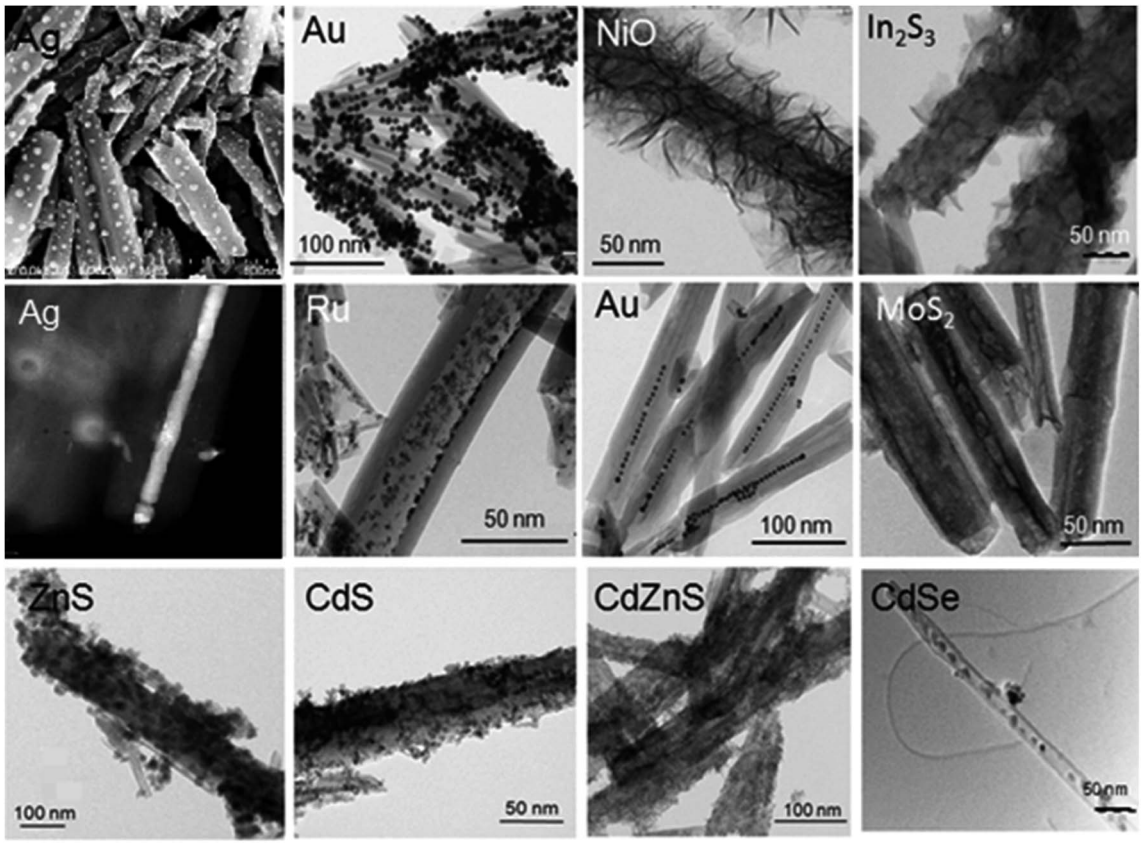

Fig. 2 Metal containing core–shell structures based on clay nanotubes, upper row – location outside: Ag, Au, NiO, and In_2S_3 – taken from ref. 29 with permission, copyright by Elsevier, 2015. Middle row – tubes loaded inside: Ag, Ru, Au, and MoS_2; bottom row – halloysite loaded inside/outside: ZnS, CdS, CdZnS, and CdSe.

sulfidation.[35] Sulfide particles of *ca.* 4.2 nm in length with an average stacking number of 1.6 were reported. The content of MoS_2 was 70 at%, and Co was 61 at%, due to the promotion of MoS_2 edges with cobalt atoms. Such a location of sulfide species in the tube inner cavity resulted in shielding the catalyst from leaching. This tubular structure does not prevent desirable mass-transfer for branched sulfur molecules that are present in a feedstock.

For useful architecture, it is essential to provide building nanoblocks with specific properties such as, for example, synthesis of monometallic Ru and bimetallic RuCo particles of 3–6 nm in diameter selectively inside the halloysite lumen.[36,37] To achieve loading of RuCo in the aluminosilicate tubes, ruthenium nanoclusters were first formed inside the clay tubes by a microwave-assisted method (Fig. 3). This was followed by cobalt ions' attraction to ruthenium during the wetness impregnation step. Reduction of Ru-salt within the lumen was the critical parameter for Fischer–Tropsch catalytic synthesis. Also, the choice of complexation agents for selective loading of Ru-particles may be used as a regulation factor for the tuning of this core–shell system's catalytic properties.

Hydrophobization of the outer clay tube surface was used for multifunctional systems working at the oil–water interface and in hydrogenation reactions with ruthenium catalysts. The external halloysite modification with alkyltriethoxysilanes enhances the hydrophobicity of the nanotubes (water contact angle up to 122°) and enables their inner lumen selective loading with 4 nm ruthenium particles. Therefore, we discussed here a strategy of halloysite core–shell system design by placing metal nanoblocks inside or outside the nanotubes, accomplished with the system's amphiphile hydrophobization allowing work in water–petroleum mixtures. The concept allows for control of metal dispersion and active phase localization depending on alkyl chain length in silanes. This prevents contact of water with the active metal phase and preserves the catalyst stability for at least 10 working cycles. Its activity was further decreased probably due to partial metal leaching (Ru-content decreased from 2.7 to 2.4 wt% after 1 cycle).[38] The activities in hydrogenation of aromatics over Ru-loaded inside the clay nanotubes and grafted outside were close, but the stability of Ru-particles located inside the nanoclay was higher. Such inner-core nanoreactors were 10–20% more active and 10-times more stable than the Ru-halloysite composite without a protective hydrophobic shell (in water–organic mixtures, the catalysts supported on non-modified halloysite were deactivated in 30 minutes).

An advantage of the inner encapsulation of catalytic nanoparticles was also demonstrated for agglomeration-tolerant Cu–Ni/halloysite systems with the interior metal alloy placement. It efficiently catalyzed motor vehicle exhaust comprising nitrogen

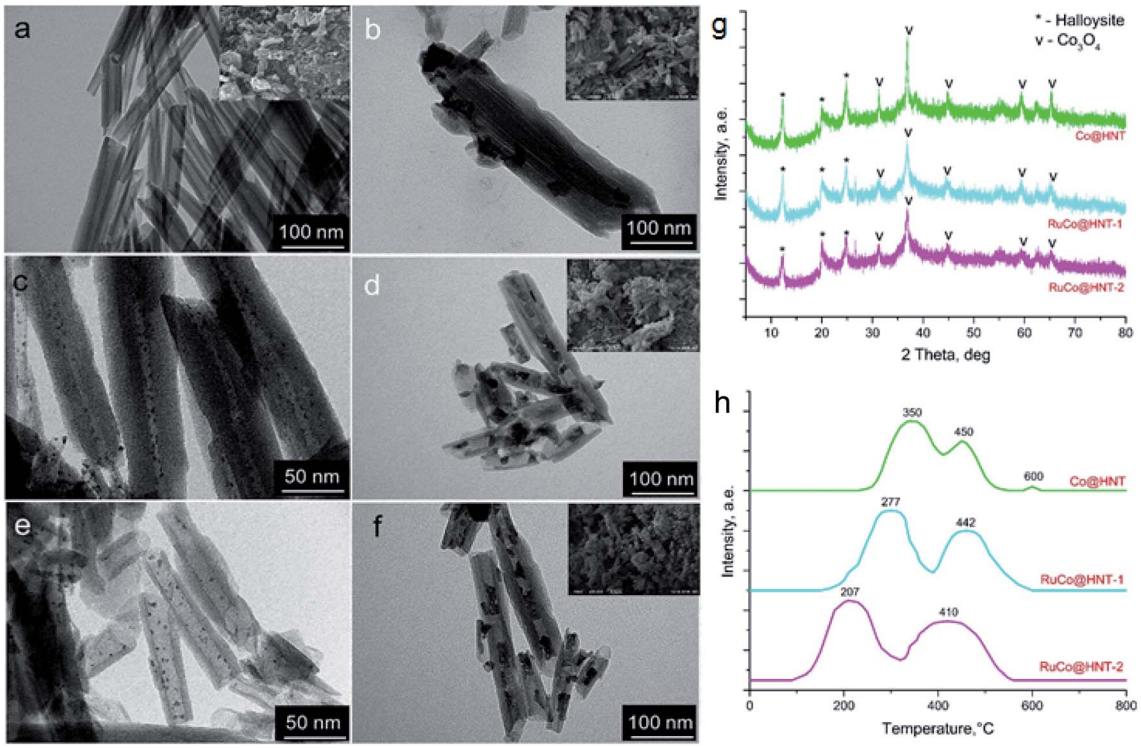

Fig. 3 (a) TEM images of monometallic Co/HNT (b) and Ru@HNT-1 (c), Ru@HNT-2 (d), bimetallic RuCo@HNT-1 (e), and RuCo@HNT-2 (f) with Ru and RuCo particles synthesized selectively inside halloysite nanotubes (HNT), (g) X-ray patterns, (h) corresponding temperature programmed reduction (TPR) curves. RuCo@HNT-1 was prepared using hydrogen as a reducing agent and RuCo@HNT-2 using $NaBH_4$ as a reducing agent for ruthenium nanoclusters, images taken from ref. 38 with permission from Elsevier, copyright 2022.

monoxide and carbon monoxide at a working temperature of *ca.* 400 °C when the activity of non-encapsulated usual catalysts was drastically decreased.[22] Similarly, efficient gas-phase halloysite core–shell nanoclay reactors could be developed for pollutant removal using two-type metal particles selectively located on the different surfaces of halloysite tubes. Therefore, the sensitivity of the halloysite nanocatalysts to metal leaching, aggregation, sintering and deactivation is controlled by the following factors: internal or external locations of the catalyst; type of interactions with the clay support surface (covalent binding and electrostatic or physical sorption), acidity and types of surface groups (hydroxyl, amino, and phosphine) of the support, and reaction conditions (temperature, liquid or gas phase process and the presence of strong acids/alkalis or water).[8]

3. Hybridization of clay nanotube systems with synthetic mesosilica

Like many natural materials, halloysite nanotubes have a relatively low surface area, acidity, and irregularities in morphology (for example, the tube diameter from different deposits may vary from 40 to 80 nm). These limit pristine halloysite's usage as a support in heterogeneous reactions, though it was already used for industrial petroleum catalytic cracking in the sixties.[7,8] These disadvantages can be overcome by the build-up of hetero-composites with tuned porosity and acidity. We introduced a strategy for the synthesis of structured mesoporous silica of MCM-41 (Mobil Composite Material-41) on the halloysite nanotube surface.[20,26] This approach involves cationic surfactant micelles' – cetyltrimethyl ammonium halide – interaction with the negatively charged outer surface of halloysite (Scheme 3). After silica precursor addition, its hydrolysis at a pH of 10–12 and aging at 90–100 °C for 20–24 hours, a well-organized silica framework was formed. The organic template was then removed by calcination in air at 550 °C, followed by the formation of structured mesoporous silica MCM-41 arrays with a thickness of *ca.* 100 nm surrounding clay nanotubes.[8,26]

This composite of MCM-41/HNT (60 wt% silica) is characterized by a much larger specific surface area; twice the mechanical strength (up to 500 MPa), and 200 °C higher thermal stability (up to 1100 °C) as compared to the bare MCM-41 catalytic material. It is due to a hierarchical composite formation, which comprises mesoporous silica reinforced with halloysite nanotubes like a durable canvas or skeleton.[26]

The inhomogeneity and morphology of different samples may be overaged by partially collapsing the halloysite structure while retaining its tubular morphology. This process forms mesoporous structures inside the lumens or, ultimately, may fully destroy the nanotubes followed by the rearranging of silica and alumina into new zeolite-like frameworks. The first strategy could be realized by pretreatment of the nanotubes with acids for alumina etching, ensuring access to silica layers from the internal cavity.[8] Such pretreatment allows for better filling of the

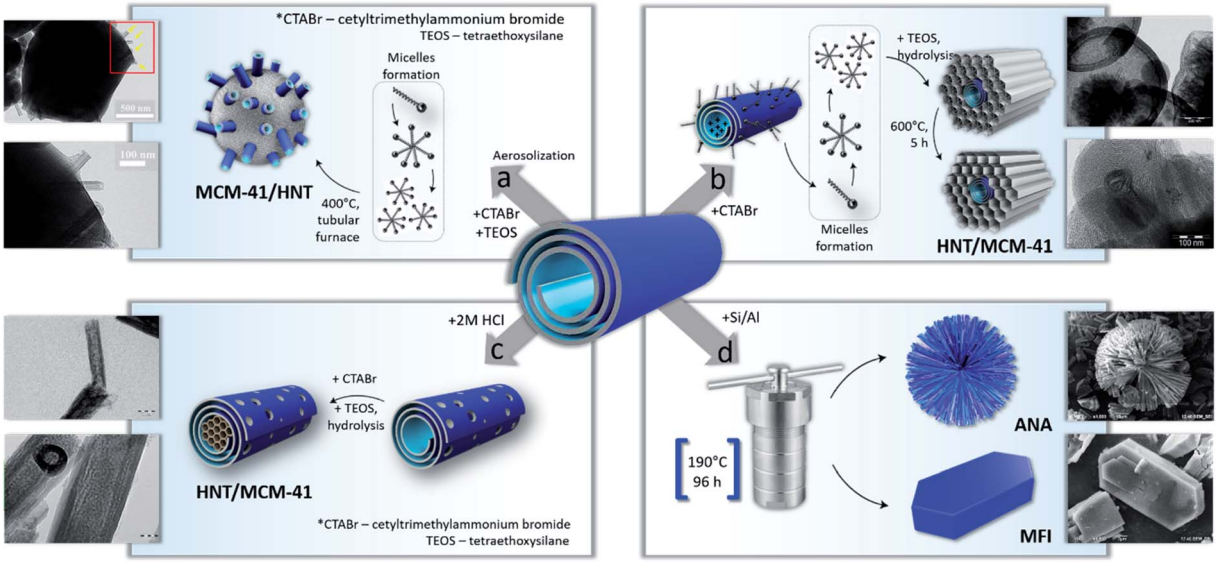

Scheme 3 Strategy for halloysite-based structured aluminosilicates synthesis: silica with poked up nanotubes (a), mesoporous silica templated onto clay nanotubes and inside the nanotubes (b and c), and bi-template synthesis of low-silica zeolite from halloysite (d).

tubes with structured mesoporous silica (Scheme 3c). The resulting composite MCM-41@HNTs also has prospects for drug delivery, and for catalysts.[8,39,40] It is characterized by an enhanced surface area of 300–400 m^2 g^{-1} and twice the acidity as compared to pristine halloysite, which may have originated from new Si–O(H)–Al bond formation and an increase in Lewis and Brønsted acid sites.

Another strategy was suggested by spray-drying a mixture containing halloysite, a cationic surfactant and tetraethoxysilane (precursors for MCM-41), Scheme 3a and Fig. 4.[25] After spray-drying, separated microparticles were collected and calcined at 550 °C to remove organics (Fig. 4a). The resulting material consists of globular *ca.* 2 μm diameter particles of MCM-41 type silica with incorporated halloysite nano-straws (Fig. 4b and c). This material has an enlarged specific surface area of 1000 m^2 g^{-1}, and its structure opens possibilities for dual encapsulation of functional molecules using clay nanotubes as transport channels.

The next strategy to create inorganic composite materials from halloysite is bi-template zeolite synthesis (Scheme 3d). Traditionally, to construct a zeolite framework one needs silicon and aluminium precursors.[41,42] We introduced a bi-template method where halloysite nanotubes were used both as a hard template and source of Al and Si. For tuning the resulting zeolite structures, traditional organic templates were employed.[43,44] We have synthesized aluminosilicates of analcime, sodalite, mordenite, and mordenite framework inverted types, allowing for highly crystalline low-silica zeolites (Fig. 5).

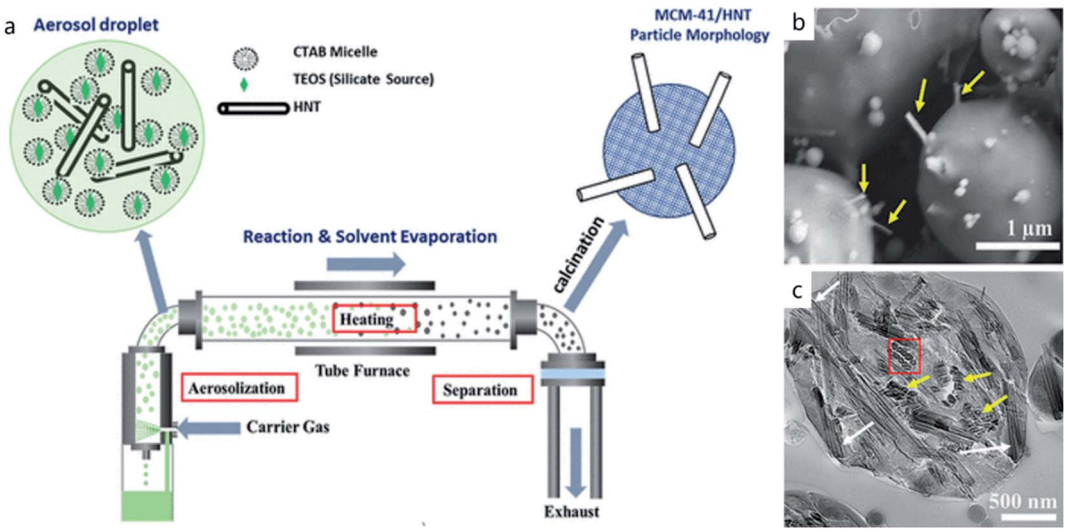

Fig. 4 Schematic illustration of the spray-drying technique (a), and SEM (b) and TEM (c) images of the resulting MCM-41/HNT particles. Adapted with permission from ref. 25 Copyright by American Chemical Society, 2022.

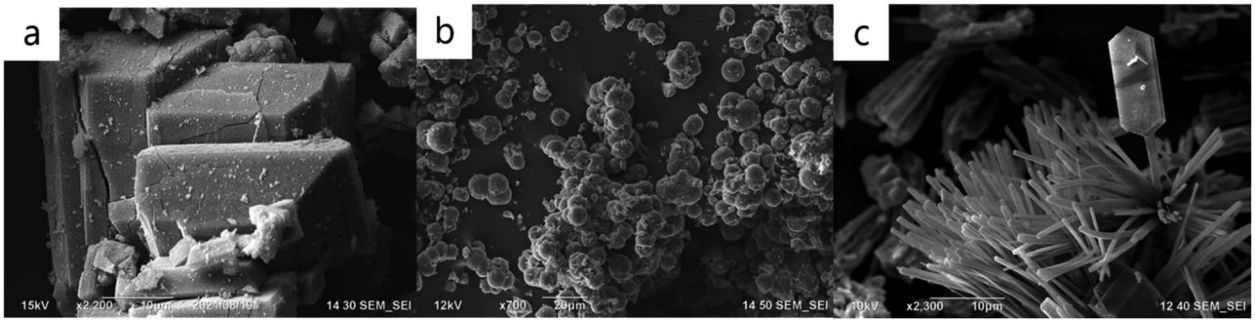

Fig. 5 SEM images of zeolites of mordenite framework inverted (a), analcime (b), and the mixture of analcime with mordenite framework inverted, all synthesized from halloysite (c).

It was shown that molar ratio adjustment of silica to alumina with gels or clay nanotube etching significantly impacts the resulting zeolite crystalline morphology (globules, hexagonal coffins, and pompon-like microfibers), while organic template variations did not have a considerable contribution.[43] Microporosity and structural variety could be beneficially broadened with silica-rich zeolite produced from halloysites with the ability to control the structural framework formation.[8,43–45]

4. Interfacial halloysite self-assembly into organized tube arrays

Formation of ordered arrays of clay nanotubes relies on their rod-like anisotropy with an axis ratio of *ca.* 1 : 20 (50 × 1000 nm) and adjustable surface charge with a zeta-potential of −30 to −60 mV, as well as on their steric interaction with shear force alignment.[46–49] In the related case of halloysite interfacial organization with direct or reversed Pickering emulsification, we have oil microbubbles–water or water droplets–air systems with the nanoclay shells.[50,51] In a simple experiment, such nanotube orientation may be observed at the edges of dried halloysite dispersion droplets. This approach allowed for capillary or surface patterning with oriented nanoclay rings located with a periodicity of *ca.* 100 μm, Scheme 4, upper row. The orientation of halloysite nanotubes in microchannels is similar to the orientation of floating wood logs down the river (Scheme 4, middle row), except that we also used the efficient clay nanotube orientation to enhance electrostatic and capillary forces with the sample drying at 65–70 °C.

When the halloysite dispersion evaporates on a solid surface, it leaves a deposit, the structure of which depends on the route of liquid evaporation. In the most common "coffee ring" deposits, liquid evaporates from the edge of the round drop, pumping liquid from the interior and transferring the nanotubes to form oriented rings. Alternating pinning and depinning processes taking place during solvent evaporation with delivery governed by the metal ball lead to the formation of concentric rings with controlled thickness and periodicity. The suspension drying out in a restricted space allows for the formation of regular patterns, as shown in Scheme 4, upper row. The structured surfaces of the oriented nanotubes enhance interactions with biological cells improving their capturing and inducing differentiation in stem cells. Interaction of these cells with halloysite also enables control of their growth and proliferation.[49] Another application of such ordered nanoclay arrays was in coating onto polyacrylonitrile porous membrane filters. The well-ordered nanotube layers allowed for excellent color rejection with high salt permeation (87% for aqueous NaCl), and thus these micro/nano composite membranes were suitable for dye purification or concentration.[7]

A similar interfacial self-assembly approach was developed for spill petroleum bioremediation exploiting mechanisms of Pickering emulsification. This process is simple, works with seawater and requires only a few minutes of shaking of a 1 wt% halloysite dispersion with a water–oil mixture. After this, stable 5–10 micrometer diameter petroleum bubbles covered with a few layers of clay nanotubes were formed. Used clay nanotubes may be additionally loaded with a standard oil dispersant, such as Corexit®, for synergetic remediation efficiency, Fig. 6a–c.[51,52] Using a natural clay dispersant instead of amphiphiles in petroleum distillates (partially, with harmful anionic ones) is environmentally friendly, and, for example, enhances proliferation of biofilm formation ("sea-snow") developed by the most common oil-eating *A. borkumensis* bacteria, Fig. 6d.[52]

Another example of spontaneous halloysite nanotube organization is its colloidal self-assembly on hair, Fig. 7.[53] Application of an aqueous 1 wt% halloysite dispersion to human hair for 2–3 minutes resulted in the formation of a 1–2 μm thick coating. This nanoclay coating is quite stable and survives seven shampoo washings, especially with partial halloysite hydrophobization. Loading these clay nanotubes with dyes or keratin allows for hair coloring or its UV protection. For such nanoclay-hair coatings, an important role is played by the surface roughness defined by the cuticle gaps, where the halloysite assembly was initiated. Probably, there is some similarity between halloysite interfacial layer formation on the oil–water and hair–air surfaces, Fig. 6c and 7c.

5. Nanoclay architecture for applications

Due to the tubular morphology and different inside/outside chemistries, halloysite, and other nanotube/nanofiber clays imogolite and sepiolite,[7] are prospective templates for

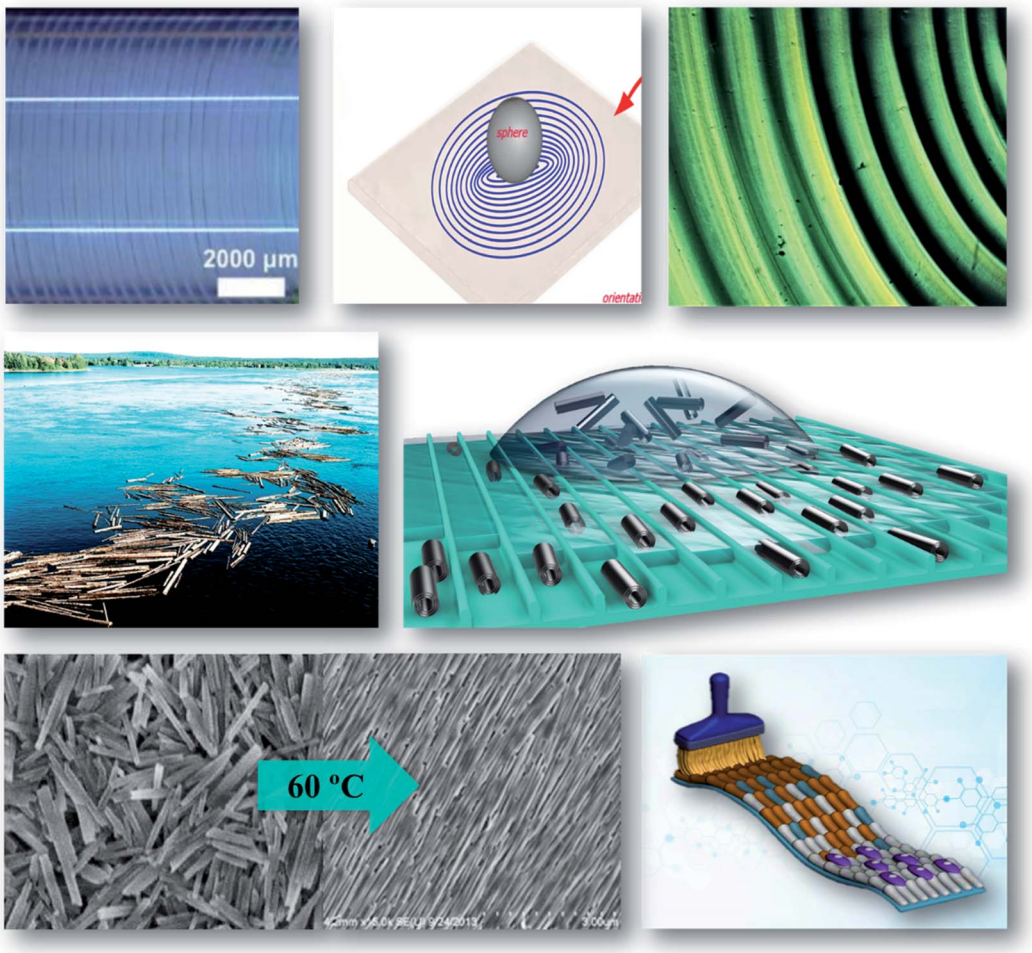

Scheme 4 Clay nanotube self-assembly, upper row: on the wall of a 1 mm diameter glass capillary, adapted from ref. 48 with permission from American Chemical Society, copyright 2016, and a similar hot-drying formation of a concentric ring after the droplet on a 2 mm diameter metal ball. Middle row: the idea borrowed from logs floating and used for halloysite orientation in microcapillaries. Bottom row: image of capillary oriented clay nanotubes dried at 60 °C and scheme of brash-orientation in coating of concentrated halloysite dispersions.

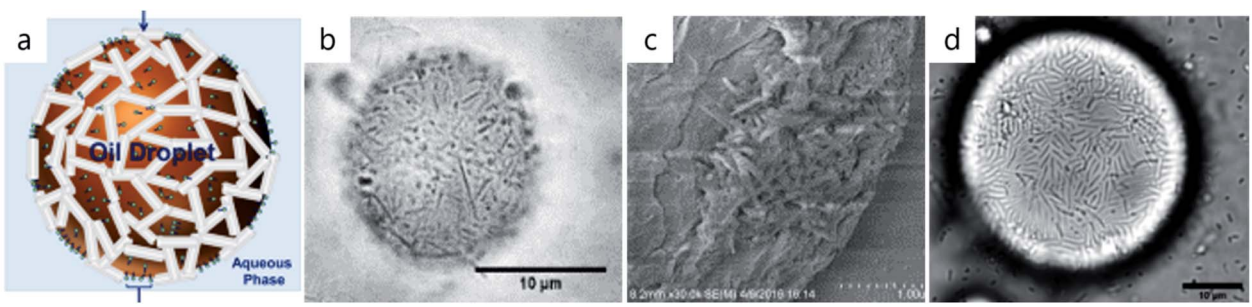

Fig. 6 Scheme of halloysite positioning onto the oil droplet (a), adapted from ref. 51 with permission from American Chemical Society, copyright 2015. Macondo crude oil halloysite emulsification, optical and cryo-SEM images (b and c), and *A. borkumensis* marine bacteria proliferation on the droplets after five days of exposure (d), (a) adapted from ref. 52 with permission from Elsevier, copyright 2018.

nanoarchitectural design of functional hybrids and organized arrays with tunable properties. These nanotubes may be loaded with drugs and chemical inhibitors, and allow for a slow release over many days (for example, 300 hours of delivery of the antibiotic ciprofloxacin). *In vitro* experiments have shown nanoclay ciprofloxacin efficiency in the treatment of drug-resistant gas gangrene bacteria *P. aeruginosa*, Fig. 8. Such halloysite-drug formulations may be delivered topically to sick body spots or, in a more complicated way, could provide targeted delivery with switchable drug release inside the cells or on their surface, as

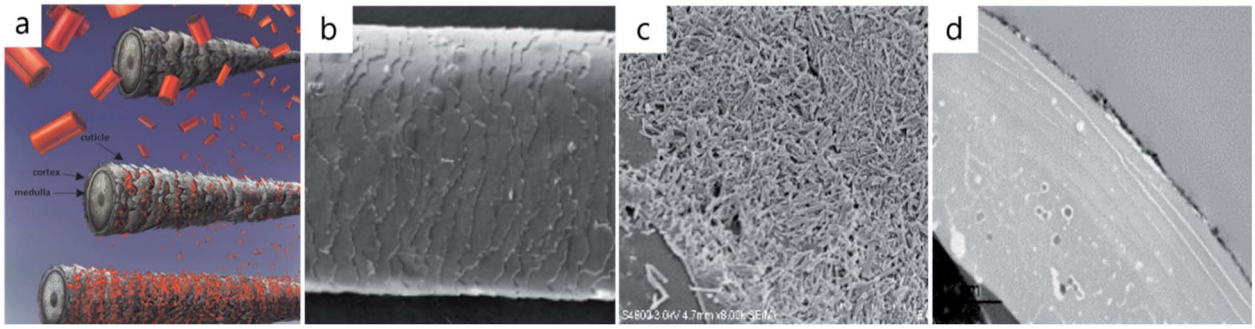

Fig. 7 Halloysite hair coating: the scheme of the process (a), SEM image of untreated human hair (b), and SEM (c) and TEM (d) cross-sectional images of the nanotube layer on hair. Adapted with permission from ref. 53 copyright by Royal Society of Chemistry, 2018.

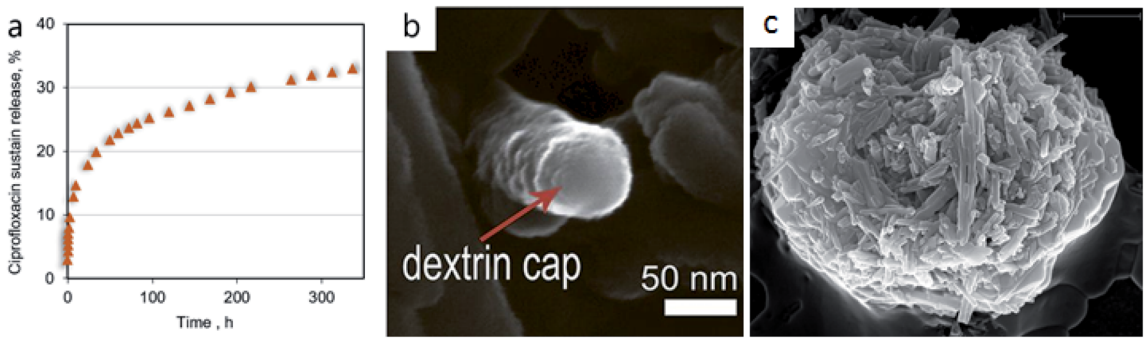

Fig. 8 Kinetics of the antibiotic ciprofloxacin's sustained release from halloysite nanotubes sealed with dextran (a), and the SEM image of the tube-end dextran cap (b) reproduced with permission from ref. 54 copyright by Springer 2015. The SEM image of the halloysite shell on the *C. pyrenoidosa* algae cell (c).

shown for the dextran capped loaded halloysite penetrating into human lung carcinoma cells, Fig. 8b.[54] Depending on the cell type, halloysites may accumulate on the surface forming a ceramic "armor" shell or penetrate inside the cell. We introduced the term "nano-torpedo" for such halloysite intracellular penetration assuming easier penetration of the loaded nanotubes through cell membranes and skin in a perpendicular position, when the efficient halloysite cross-section may be compared with 50 nm diameter spherical nanoparticles.[55] Practically, for medical skin applications this may be performed by halloysite-cream massaging.

Halloysite nanoclay was self-assembled on live microbial or algae cells, Fig. 8c. The clay nanotubes were coated with a polycation and then deposited on the oppositely charged *Chlorella pyrenoidosa* algae cells. Structurally, the hybrid cell/clay microparticles are quite similar to the oil droplets coated with halloysite. However, here electrostatic interactions are the main driving forces to produce and maintain the integrity of the shells, while in oil emulsifications, stability is based on interfacial hydrophilic/hydrophobic balance. Potentially, self-assembly on live cells may be utilized for the fabrication of biocatalysts or drug delivery vehicles.

Including drug loaded halloysite in bone cement or for wound tissue healing gels allowed for extended (two weeks) antibacterial treatments. Halloysite embedded at 5–8 wt% in chitosan/gelatin gels provides a biocompatible ceramic skeleton for wound dressing essentially accelerating the healing process. These halloysite scaffolds showed excellent resorption within six weeks after implantation in the rat wound: neo-vascularization was observed in the newly formed connective tissue allowing for the restoration of blood flow.[9,10]

In metal–ceramic core–shell systems, halloysite clay nanotubes enable selective placement of the active phase (Co, Ru, Mo, Pt, Ni, and Ag) inside or outside the tubes depending on the target reaction or conditions. The unique tubular morphology allows for metals to be embedded in the lumen while the outer halloysite surface may be covered with modifiers, *e.g.* hydrophobized with silanes to prevent interaction of the active phase with water, thus avoiding leaching and deactivation of the catalyst. Such a strategy may be applied to catalytic hydrogenation/hydrodeoxygenation, dibenzothiophene hydrodesulphurization, and Fischer–Tropsch synthesis.[36,39,56] This approach may be transposed to oil refining processes such as hydrotreating of middle distillates and vacuum gasoil, hydroupgrading of water-containing bio-oils, synthetic oils and clean components of motor fuels from syngas. Another prospective field for application of halloysite nanocomposites may be attributed to hydrogen storage with aminoboranes and catalytic nanoparticles allowing for on-demand release (Scheme 5).

Core–shell composite materials with structured mesoporous MCM-41 silica covered or embedded in the nanotubes are prospective for photocatalysis, hydrotreating processes, sulfur

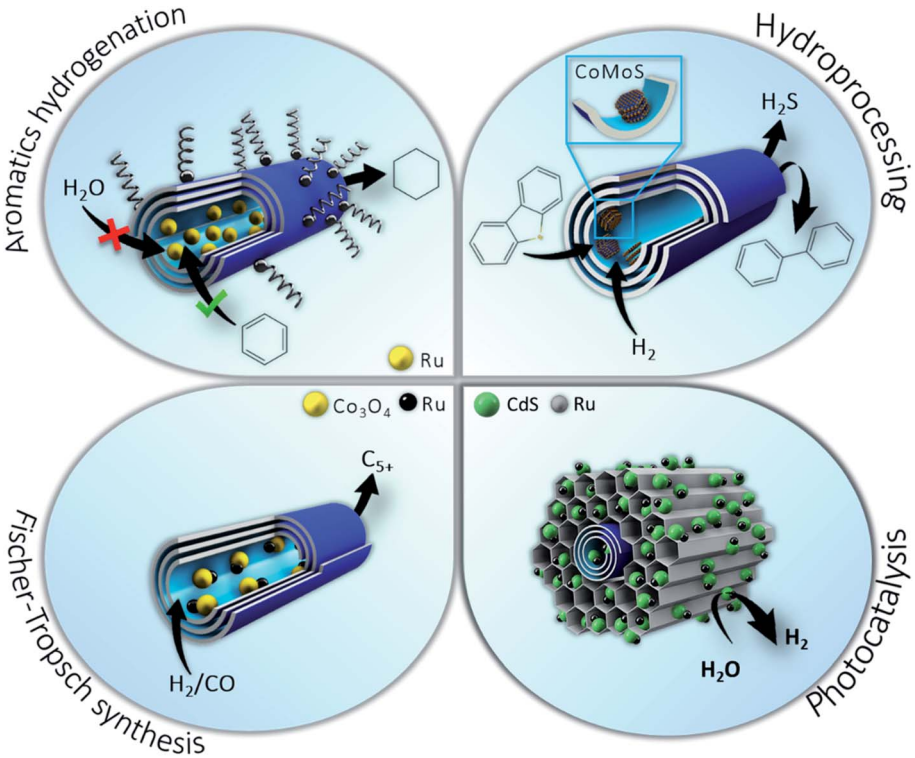

Scheme 5 Nanoreactors templated on clay nanotubes for catalytic hydrogenation of aromatics in water media, dibenzothiophene hydrodesulphurization, and Fischer–Tropsch synthesis and photocatalysis.

reduction additives for FCC (fluid catalytic cracking) and CO_2 capturing.[8,26,36,57] High surface area, tunable pore-size distribution, mild acidity and controlled morphology are the key factors for boosting nanoclay research and development for oil refining and decarbonization. This may be extended by tuning halloysite acidity with etching, which helps to improve the acid-catalyzed C–S bond scission and C–C isomerization.[35,58] We confirmed retaining the nanotubular structure after extrusion with a boehmite binder and for composites with silica followed by its calcination.[36] Halloysite is an aluminosilicate clay available in thousands of tons at a low price, and it may be used as a silica and alumina source for industrial zeolites with a desirable porous framework, textural properties, and acidity. Besides, this tubular nanoclay allows for mesoporous aluminosilicate design, exploiting a cheaper synthesis route.

In conclusion, one can construct functional core–shell clay nanotube systems with active inner load (metals, drugs and chemical inhibitors) confined in the lumens, accomplished with the outside buildup of other elements, such as silanes and amphiphiles, and disperse them in water, oil gels or medical formulations with controlled delivery for wound healing, petroleum and other organic catalysis, or protective coating (anticorrosion, flame retardant, and antifouling). In the second architectural step, one could assemble such nanotube heterosystems into organized interfacial arrays for spill oil remediation, microemulsion reactors, shells on microorganisms, and in oriented biomedical systems for cell capturing and stem cell differentiation. This is prospective for integrated nano/micro robotic systems combining ceramic, metallic and biological components for the most efficient functionality.

Conflicts of interest

There are no conflicts of interest to declare.

References

1 K. Ariga, X. Jia, J. Song, J. Hill, D. Leong, Y. Jia and J. Li, Nanoarchitectonics beyond Self-Assembly: Challenges to Create Bio-Like Hierarchic Organization, *Angew. Chem.*, 2020, **59**, 15424–15446.
2 K. Ariga, Y. Lvov and G. Decher, There is still plenty of room for layer-by-layer assembly for constructing nanoarchitectonics-based materials and devices, *Phys. Chem. Chem. Phys.*, 2022, **24**, 4097.
3 K. Chatterjee, S. Sarkar, K. J. Rao and S. Paria, Core/shell nanoparticles in biomedical applications, *Adv. Colloid Interface Sci.*, 2014, **209**, 8–39.
4 X. Ji, R. Shao, A. Elliott, R. J. Stafford, E. Esparza-Coss, J. Bankson, G. Liang, Z.-P. Luo, K. Park, J. Markert and C. Li, Bifunctional Gold Nanoshells with a Superparamagnetic Iron Oxide-Silica Core Suitable for MR Imaging and Photothermal Therapy, *J. Phys. Chem. C*, 2007, **111**, 6245–6251.
5 M. Liu, Z. Jia, D. Jia and C. Zhou, Recent advance in research on halloysite nanotubes-polymer nanocomposite, *Prog. Polym. Sci.*, 2014, **39**, 1498.

6 G. Cavallaro, G. Lazzara and S. Milioto, Exploiting the Colloidal Stability and Solubilization Ability of Clay Nanotubes/Ionic Surfactant Hybrid Nanomaterials, *J. Phys. Chem. C*, 2012, **116**, 21932.

7 Y. Lvov, W. Wang, L. Zhang and R. Fakhrullin, Halloysite Clay Nanotubes for Loading and Sustained Release of Functional Compounds, *Adv. Mater.*, 2016, **28**, 1227–1250.

8 A. Glotov, A. Vutolkina, A. Pimerzin, V. Vinokurov and Y. Lvov, Clay nanotube-metal core/shell catalysts for hydroprocesses, *Chem. Soc. Rev.*, 2021, **50**, 9240–9277.

9 G. Lazzara, G. Cavallaro, V. Vinokurov, R. Fakhrullin, A. Stavitskaya, A. Panchal and Y. Lvov, Self-assembly of organic-inorganic composites using halloysite clay nanotubes, *Curr. Opin. Colloid Interface Sci.*, 2018, **35**, 42–50.

10 A. Santos, I. Pereira, F. Veiga, S. Reis, M. Saleh and Y. Lvov, Biomedical potential of clay nanotube formulations and their toxicity assessment, *Expert Opin. Drug Delivery*, 2019, **16**, 1169–1182.

11 R. Qi, R. Guo, F. Zheng, H. Liu, J. Yu and X. Shi, Controlled release and antibacterial activity of antibiotic-loaded electrospun halloysite/poly(lactic-co-glycolic acid) composite nanofibers, *Colloids Surf., B*, 2013, **110**, 148–155.

12 M. Kryuchkova, A. Danilushkina, Y. Lvov and R. Fakhrullin, Evaluation of toxicity of nanoclays and graphene oxide in vivo: Paramecium caudatum study, *Environ. Sci.: Nano*, 2016, **3**, 442–452.

13 R. Rong, Y. Zhang and Y. Zhang, Inhibition of inhaled halloysite nanotube toxicity by trehalose through enhanced autophagic clearance of p62, *Nanotoxicology*, 2019, **3**, 354–368.

14 X. Wang, J. Gong, Z. Gui, T. Hu and X. Xu, Halloysite nanotubes-induced Al accumulation and oxidative damage in liver of mice after 30-day repeated oral administration, *Environ. Toxicol.*, 2018, **33**, 623–630.

15 J. Tully, R. Yendluri and Y. Lvov, Enzyme Stabilization by Immobilization Onto and Into Clay Nanotubes, *Biomacromolecules*, 2016, **17**, 615–621.

16 D. Shchukin, R. Price and Y. Lvov, Biomimetic Synthesis of Vaterite in the Interior of Clay Nanotubules, *Small*, 2005, **1**, 510–513.

17 M. Massaro, G. Cavallaro, C. Colletti, G. Lazzara, S. Milioto, R. Noto and S. Riela, Chemical modification of halloysite nanotubes for controlled loading and release, *J. Mater. Chem. B*, 2018, **6**, 3415.

18 A. Abu El-Soad, A. Pestova, D. Tambasova, V. Osipova, N. Martemyanova, G. Cavallaro, E. Kovaleva and G. Lazzara, Insights into grafting of (3-Mercaptopropyl) trimethoxy silane on halloysite nanotubes surface, *J. Organomet. Chem.*, 2020, **915**, 121224.

19 C. Taş, S. Gundogdu and H. Ünal, Clay-based Controlled Release System for Sunlight triggered, *ACS Appl. Nano Mater.*, 2022, **5**, 5407–5415.

20 V. Vinokurov, A. Glotov, Y. Chudakov, A. Stavitskaya, E. Ivanov, A. Zolotukhina, A. Maximov, E. Karakhanov, W. Huang and Y. Lvov, Mesoporous metal catalysts templated on clay nanotubes, *Bull. Chem. Soc. Jpn.*, 2019, **92**, 61–69.

21 T. Rostamzadeh, S. I. Khan, K. Riche, A. Stavitskaya, Y. Lvov and J. Wiley, Rapid and Controlled In-Situ Growth of Noble Metal Nanostructures within Halloysite Nanotubes, *Langmuir*, 2017, **33**, 13051–13059.

22 N. Sanchez-Ballester, G. Ramesh, T. Tanabe, L. Shrestha, E. Koudelkova, Y. Lvov, K. Ariga and H. Abe, Activated Interior of Clay Nanotubes for Agglomeration-tolerant Exhaust Purification, *J. Mater. Chem.*, 2015, **3**, 6614–6619.

23 G. Cavallaro, G. Lazzara, S. Milioto, F. Parisi, V. Evtugyn, E. Rozhina and R. Fakhrullin, Nanohydrogel Formation within the Halloysite Lumen for Triggered and Sustained Release, *ACS Appl. Mater. Interfaces*, 2018, **10**, 8265–8273.

24 S. Sadjadi, M. Malmir, G. Lazzara, G. Cavallaro and M. Heravi, Preparation of palladated porous nitrogen-doped carbon using halloysite as porogen: disclosing its utility as a hydrogenation catalyst, *Sci. Rep.*, 2020, **10**, 2039.

25 A. Farinmade, O. Ajumobi, L. Yu, Y. Su, Y. Zhang, Y. Lou, J. Valla and V. John, Tubular Clay Nano-Straws in Ordered Mesoporous Particles Create Hierarchical Porosities Leading to Improved CO_2 Uptake, *Ind. Eng. Chem. Res.*, 2022, **61**, 1694–1703.

26 A. Glotov, N. Levshakov, A. Stavitskaya, M. Artemova, P. Guschin, E. Ivanov, V. Vinokurov and Y. Lvov, Templated self-assembly of ordered mesoporous silica on clay nanotubes, *Chem. Commun.*, 2019, **55**, 5507–5510.

27 S. Koh, Strategies for controlled placement of nanoscale building blocks, *Nanoscale Res. Lett.*, 2007, **2**, 519–545.

28 N. Li, J. Zhou, J. Yu, Y. Liu, J. Tang and W. Tang, Halloysite nanotubes favored facile deposition of nickel disulfide on NiMn oxides nanosheets for high-performance energy storage, *Electrochim. Acta*, 2018, **273**, 349–357.

29 J. Liang, H. Tan, C. Xiao, G. Zhou, S. Guo and S. Ding, Hydroxyl-riched halloysite clay nanotubes serving as substrate of NiO nanosheets for high-performance supercapacitor, *J. Power Sources*, 2015, **285**, 210–216.

30 A. Stavitskaya, E. Kozlova, A. Kurenkova, A. Glotov, D. Selischev, E. Ivanov, D. Kozlov, V. Vinokurov, R. Fakhrullin and Y. Lvov, Ru/CdS Quantum Dots Templated on Clay Nanotubes as Visible-Light-Active Photocatalysts: Optimization of S/Cd Ratio and Ru Content, *Chem.–Eur. J.*, 2021, **26**(57), 13085–13092.

31 A. Stavitskaya, A. Novikov, M. Kotelev, D. Kopitsyn, E. Rozhina, I. Ishmukhametov, R. Fakhrullin, E. Ivanov, Y. Lvov and V. Vinokurov, Fluorescence and cytotoxicity of cadmium sulfide quantum dots stabilized on clay nanotubes, *Nanomaterials*, 2018, **8**(6), 391.

32 A. Stavitskaya, G. Fakhrullina, L. Nigamatzyanova, E. Sitmukhanova, E. Khusnetdenova, R. Fakhrullin and V. Vinokurov, Biodistribution of Quantum Dots-Labelled Halloysite Nanotubes: A Caenorhabditis elegans In Vivo Study, *Materials*, 2021, **14**(19), 5469.

33 B. Micó-Vicent, F. M. Martínez-Verdú, A. Novikov, A. Stavitskaya, V. Vinokurov, E. Rozhina, R. Fakhrullin, R. Yendluri and Y. Lvov, Stabilized dye–pigment formulations with platy and tubular nanoclays, *Adv. Funct. Mater.*, 2018, **28**(27), 1703553.

34 L. Lisuzzo, G. Cavallaro, S. Milioto and G. Lazzara, Halloysite nanotubes as nanoreactors for heterogeneous micellar catalysis, *J. Colloid Interface Sci.*, 2022, **608**, 424–434.
35 A. Pimerzin, A. Vutolkina, N. Vinogradov, V. Vinokurov, Y. Lvov and A. Glotov, Core-shell catalysts with CoMoS phase embedded in clay nanotubes for dibenzothiophene hydrodesulfurization, *Catal. Today*, 2022, DOI: **10.1016/j.cattod.2021.11.019**.
36 A. Stavitskaya, K. Mazurova, M. Kotelev, O. Eliseev, P. Gushchin, A. Glotov, R. Kazantsev, V. Vinokurov and Y. Lvov, Ruthenium-Loaded Halloysite Nanotubes as Mesocatalysts for Fischer–Tropsch Synthesis, *Molecules*, 2020, **25**, 1764.
37 K. Mazurova, A. Glotov, M. Kotelev, O. Eliseev, P. Gushchin, M. Rubtsova, A. Vutolkina, R. Kazantsev, V. Vinokurov and A. Stavitskaya, Natural aluminosilicate nanotubes loaded with RuCo as nanoreactors for Fischer-Tropsch synthesis, *Sci. Technol. Adv. Mater.*, 2022, **23**, 17–30.
38 A. Glotov, A. Novikov, A. Stavitskaya, V. Nedolivko, D. Kopitsyn, A. Kuchierskaya, E. Ivanov, V. Stytsenko, V. Vinokurov and Y. Lvov, Nanoreactors based on hydrophobized tubular aluminosilicates decorated with ruthenium: Highly active and stable catalysts for aromatics hydrogenation, *Catal. Today*, 2021, **378**, 33–42.
39 L. Fu, H. Yang, A. Tang and Y. Hu, Engineering a tubular mesoporous silica nanocontainer with well-preserved clay shell from natural halloysite, *Nano Res.*, 2017, **10**, 2782–2799.
40 Z. Shua, Y. Chen, J. Zhou, T. Li, Z. Sheng, Ch. Tao and Y. Wang, Preparation of halloysite-derived mesoporous silica nanotube with enlarged specific surface area for enhanced dye adsorption, *Appl. Clay Sci.*, 2016, **132–133**, 114–121.
41 J. Li, A. Corma and J. Yu, Synthesis of new zeolite structures, *Chem. Soc. Rev.*, 2015, **44**, 7112–7127.
42 I. Ivanova and E. Knyazeva, Micro-Mesoporous Materials Obtained by Zeolite Recrystallization: Synthesis, Characterization and Catalytic Applications, *Chem. Soc. Rev.*, 2013, **42**, 3671–3688.
43 M. Rubtsova, E. Smirnova, S. Boev, M. Kotelev, K. Cherednichenko, V. Vinokurov and Y. Lvov, Aleksandr Glotov, Nanoarchitectural approach for synthesis of highly crystalline zeolites with a low Si/Al ratio from natural clay nanotubes, *Microporous Mesoporous Mater.*, 2022, **330**, 11622.
44 M. Meftah, W. Oueslati, N. Chorfi and A. Ben Haj Amara, Effect of the raw material type and the reaction time on the synthesis of halloysite based Zeolite Na-P1, *Results Phys.*, 2017, **7**, 1475–1484.
45 A. Sadovnikov, O. Arapova, V. Russo, A. Maximov, D. Murzin and E. Naranov, Synergy of Acidity and Morphology of Micro-Mesoporous Materials in the Solid-Acid Alkylation of Toluene with 1-Decene, *Ind. Eng. Chem. Res.*, 2022, **61**, 1994–2009.
46 Y. Lvov, A. Panchal, Y. Fu, R. Fakhrullin, M. Kryuchkova, S. Batasheva, A. Stavitskaya and V. Vinokurov, Interfacial self-assembly in halloysite nanotube composites, *Langmuir*, 2019, **35**, 8646–8657.
47 Z. Q. Luo, H. Z. Song, X. R. Feng, M. T. Run, H. H. Cui, L. C. Wu, J. G. Gao and Z. G. Wang, Liquid Crystalline Phase Behavior and Sol-Gel Transition in Aqueous Halloysite Nanotube Dispersions, *Langmuir*, 2013, **29**, 12358–12366.
48 M. Liu, R. He, J. Yang, W. Zhao and C. Zhou, Stripe-like Clay Nanotubes Patterns in Glass Capillary Tubes for Capture of Tumor Cells, *ACS Appl. Mater. Interfaces*, 2016, **8**, 7709–7719.
49 X. Zhao, C. Zhou, Y. Lvov and M. Liu, Clay nanotube aligned with shear forces for mesenchymal stem cells patterning, *Small*, 2019, **15**, 1900357.
50 O. Owoseni, E. Nyankson, Y. Zhang, S. J. Adams, J. He, G. L. Mcpherson, A. Bose, R. B. Gupta and V. T. John, Release of Surfactant Cargo from Interfacially-Active Halloysite Clay Nanotubes for Oil Spill Remediation, *Langmuir*, 2014, **30**, 13533–135441.
51 O. Owoseni, Y. Zhang, Y. Su, J. He, G. McPherson, A. Bose and V. John, Tuning the Wettability of Halloysite Clay Nanotubes by Surface Carbonization for Optimal Emulsion Stabilization, *Langmuir*, 2015, **31**, 13700–13707.
52 A. Panchal, L. Swientoniewski, T. Yu, D. Zhang, D. Blake, M. Omarova, V. John and Y. Lvov, Bacterial proliferation on clay nanotube Pickering emulsions for oil spill bioremediation, *Colloids Surf., B*, 2018, **134**, 27–33.
53 A. Panchal, G. Fakhrullina, R. Fakhrullin and Y. Lvov, Clay nanotube hair self-assembly coating for coloring and drug delivery, *Nanoscale*, 2018, **10**, 18205–18216.
54 M. Dzamukova, E. Naumenko, A. Badrutdinov, Y. Lvov and R. Fakhrullin, Enzyme-activated intracellular drug delivery with tubule clay nanoformulation, *Sci. Rep.*, 2015, **5**, 10560.
55 M. Saleh, N. Prajapati, A. Karan, A. Stavitskaya, M. Decoster and Y. Lvov, Halloysite Nanotube Vehicles for Drug Delivery through Brain Endothelial Barrier, *Clay Clay Miner.*, 2021, **69**, 603–611.
56 V. Vinokurov, A. Glotov, Y. Chudakov, A. Stavitskaya, E. Ivanov, P. Gushchin, A. Zolotukhina, A. Maximov, E. Karakhanov and Y. Lvov, Core/Shell Ruthenium–Halloysite Nanocatalysts for Hydrogenation of Phenol, *Ind. Eng. Chem. Res.*, 2017, **56**, 14043–14052.
57 A. Stavitskaya, A. Glotov, F. Pouresmaeil, K. Potapenko, E. Sitmukhanova, K. Mazurova, E. Ivanov, E. Kozlova, V. Vinokurov and Y. Lvov, Hierarchical MCM-41 templated on clay nanotubes as a support for CdS QDs and their catalytic activity in hydrogen production, *ACS Appl. Nano Mater.*, 2022, **5**, 605–614.
58 A. Glotov, A. Vutolkina, M. Artemova, N. Demikhova, E. Smirnova, E. Roldugina, A. Stavitskaya, E. Ivanov, S. Egazar'yants and V. Vinokurov, Micro-mesoporous MCM-41/ZSM-5 supported Pt and Pd catalysts for hydroisomerization of C-8 aromatic fraction, *Appl. Catal., A*, 2020, **603**, 117764.